



Semnan University



A Comparison of Catalyst Behavior of Samaria Modified Ni Catalyst Supported on Mesoporous Silica and Carbon for Methane CO₂ Reforming

Zahra Taherian^a, Mardali Yousefpor^{*a}, Mohammad Tajally^a, Behnam Khoshandam^b

^a Faculty of Materials and Metallurgical Engineering, Semnan University, Semnan, Iran.

^b Faculty of Oil, Gas and Chemical Engineering, Semnan University, Semnan, Iran.

PAPER INFO

Paper history:

Received: 2020-06-22

Revised: 2021-05-22

Accepted: 2021-05-23

Keywords:

Carbon mesostructured;
CO₂ reforming of CH₄;
Samaria, Nickel;
Silica mesostructured.

ABSTRACT

The Samaria-promoted of 10wt% Nickel-CMK-3 and 10wt% Nickel-SBA-15 were synthesized by the Samarium (3wt %) addition, and using the two-solvent impregnation technique. The N₂ adsorption-desorption, field emission scanning electron microscopy, energy dispersive x-ray analysis, x-ray diffraction and the transmission electron microscopy analysis were used to characterize of the Samaria modified and unmodified catalysts. Furthermore, the catalyst performances were tested under the carbon dioxide reforming of methane. As a result, the x-ray diffraction and surface area investigation revealed that the addition of Samaria (Sm₂O₃) into the Nickel (Ni) catalysts/silica (SBA-15) and carbon (CMK-3) mesostructures decreased the particles size and surface area according to the TEM micrographs; however, mproved the catalysts activity and catalysts stability. The role of investigation of support in the dry reforming reaction indicated that the activity and catalysts stability of the Ni/CMK-3 catalysts were lower than the Ni/SBA-15 catalysts due to the agglomeration of Ni nanoparticles on the CMK-3 support, the sintering of Ni nanoparticles, the burning of the mesoporous carbon support in the higher temperatures and the blocking of Ni nanoparticles into the deposited carbon nanotubes (CNTs).

DOI: 10.22075/JHMTR.2021.20684.1288

© 2021 Published by Semnan University Press. All rights reserved.

1. Introduction

In recent years, methane reforming in expose to carbon dioxide (CO₂) has extensively studied due to the syngas production or production of syngas [1-5]. In this reaction, methane (CH₄) and CO₂ (unfavorable greenhouse gases) are transformed into the precious products that can used to produce the different chemicals such as higher alkanes and oxygenates [6-10]. The fast deactivation of catalysts in carbon dioxide reforming of methane is the main obstacle at the industrial applications. The noble metal catalysts of Rh, Pd, La, Zr, Ru and Ir have successfully examined for this reaction without carbon deposition and the fast deactivation [11, 12]. However, the Nickel-based (Ni) catalysts are preferred to the high cost noble metals due to having the low price and more activity for CO₂ reforming [13-15]. On the other hand, the carbon materials as a catalyst or the catalyst barrier in this reaction have also been applied instead of metal-based catalysts due to the

their porosity or oxygen surface groups that can be effective on the catalysts activity and selectivity [16-21]. Consequently, a great group of carbon materials are containing carbon blacks, activated carbons, chars from biomass residues, etc. [22-25], that have examined as catalysts, for methane decomposition. The carbon-based catalysts have more benefits than the metal catalysts, because of their specific properties for example, availability, resistance, high temperature resistance, and low cost [26, 27]. In 2010, Menéndez *et al.* [16] studied the various carbons in the field of methane reforming in expose of carbon dioxide, and their results indicated that the microwave heating for carbons oxidizing leads to unfavorable catalysts. For this reason, Goscianska *et al.* [28], applied La and Ce/CMK-3 as catalysts for the CO₂ reforming of CH₄. They reported the synthesis of carbon mesostructure using the KIT-6, and SBA-15 as hard mesosilica templates. The durability time, and activity of

*Corresponding Author: Mardali Yousefpor, Faculty of Materials Science and Metallurgical Engineering, Semnan University, Semnan, Iran.

Email: myousefpor@semnan.ac.ir

La and Ce catalysts over the CMK-3 were higher than similar catalysts over the KIT-6, and SBA-15 matrix. Despite the researches in the field of carbon catalysts, no catalysts of Ni/CMK-3 have reported in the dry reforming of methane. Therefore, in the present study was investigated and focused on the Nickel catalysts with and without Samaria (Sm_2O_3) supported on CMK-3 in carbon dioxide reforming of the methane process and then compared to the Nickel catalysts with/without 3% Samaria supported on SBA-15, which was optimized in the previous our work. In this case, in this research we focused on the effect of promoter of Sm_2O_3 on the physicochemical properties of Nickel catalysts with and without Samaria (Sm_2O_3) supported on CMK-3 catalyst and their catalytic performance with the different feed ratio in steam reforming of methane for hydrogen production in compare to the Nickel catalysts with/without 3% Samaria supported on SBA-15. For reaching to this purpose, the physical and chemical properties of catalysts were evaluated by BET, XRD, HR-TEM, and FE-SEM methods.

2. Experimental route

2.1. Precursor materials

For synthesis, $\text{Ni}(\text{NO}_3)_2 \cdot 6\text{H}_2\text{O}$ and $\text{Sm}(\text{NO}_3)_3 \cdot 6\text{H}_2\text{O}$ salts prepared from Merck Company. To prepare the supports of catalysts, sucrose, TEOS (Merck, P99%), P123 ($M=5800$, Aldrich) and HCL used as well.

2.2. Synthesis of SBA-15

In the present study, the ordered hexagonal SBA-15 with uniform channels was synthesized in the strong acidic environment by hydrothermal procedure [29] as follows: Initially, 8.0 g triblock copolymer was dissolved in 60 mL of deionized water and 240 mL of hydrochloric acid 2 M and it was diluted with deionized water to reach a final volume of 300 mL. In the further step, 17 g of silica precursor was poured dropwise to the solution at 313 K and stirred vigorously for 24 h. Then, the blend was transferred to a sealed teflon vessel and heated to 373 K for 24 h. After that, the precipitated powders were centrifuged, washed and dried at 363 K for 12 h. Finally, the calcination for removing soft template was done at 773 K in air for 6 h.

2.3. Template synthesis of carbon mesostructured

The replication technique was used to the synthesis of ordered mesostructure carbon (CMK-3). The SBA-15 was applied as a hard template according to Ryoo *et al.* method [30]. As detail, 2.0 g of silica template was dispersed to the solution, which is including 2 g. sucrose, 0.28 g sulfuric acid and, 10 g deionized water. The mixture was heated at 373 K for 6 h. After that, the temperature was increased to 433 K, and kept for 6 h. The silica sample was treated again simultaneously with addition of 1.6 g sucrose, 0.18 g H_2SO_4 , and 10 g H_2O in the same drying condition. To completing the carbonization, the obtained sample was

calcined at 1273 K for 6 h under the Ar atmosphere with a stream rate of 170 mL/min. The mesosilica template was eliminated by hydrofluoric acid (5 wt%) at room temperature. Finally, carbon mesostructure was centrifuged, washed and heated at 378 K for 12 h.

2.4. Catalysts synthesis

The Nickel catalysts were prepared through the two-solvent impregnation method [31, 32]. Initially, the Nickel nitrate hexahydrate was solved in the deionized water, and added to the hexane mixture, which is containing a certain amount of mesoporous silica or carbon supports. Each mixture stirred for 2 h, and then filtered and dried at 373 K for removing the water. The impregnated samples were calcined for 3 h at 723 K. For incorporation of Samarium, the Samarium nitrate hexahydrate was impregnated to the Ni catalysts with the same procedure. Fig. 1 presents a scheme of Sm/Ni catalysts. The samples were labeled as Ni-SBA-15, Ni-CMK-3, $3\text{Sm}_2\text{O}_3\text{-Ni-SBA-15}$, and $3\text{Sm}_2\text{O}_3\text{-Ni-CMK-3}$.

2.5. Catalysts characterization

The catalysts and promoters crystalline phase have been recorded by X-ray diffraction (XRD) using a Bruker D8 diffractometer, the source of x-ray is created using the Cu-K α radiation with $\lambda=0.15418$ nm, and performed at 40 kV and 30 mA. A MIRA3 TESCAN-XMU electron scanning microscopy with EDAX detector and transmission electron microscopy, Tecnai 20 TEM from FEI Company were used to study the materials morphology. For preparing the TEM samples, a suspension of catalysts materials in the alcohol solution was ultrasonically prepared and thus, a drop of the suspension was poured on the holey carbon layer grid and dried.

An automated BEL sorp mini-II surface area analyzer was used to measure the N_2 adsorption and desorption isotherms of all catalysts at 77 K. The specific surface area calculations were done by Brunauer-Emmett-Teller (BET) technique. The diameter and the volume of pores were calculated from the adsorption branch of isotherm curves using the conventional Barrett-Joyner-Halenda (BJH)

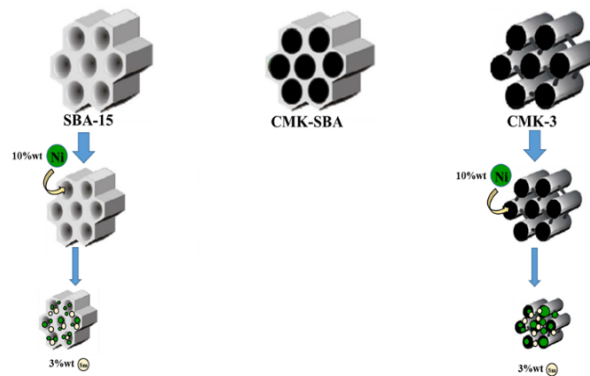


Figure 1. Scheme of synthesis of Sm_2O_3 -promoted Ni catalysts supported on SBA-15 and CMK-3.

method. Before each test, catalysts were outgassed at 423 K for 3 h. The coke formation on the surface of the used catalysts was characterized by using of Zeiss-EM10C-100 kV TEM from Germany.

2.6. Precursor materials

The activity data of the unused samples were examined in a fixed-bed continuous-flow reactor made of quartz with a diameter equal to 8 mm at 1 atm. The center of reactor was charged with 0.2g prepared catalyst and maintained by glass wool. The reaction was started by reducing sampling, when the reactant feed ($\text{CH}_4:\text{CO}_2 = 1:1$) was injected into the reactor at the different temperatures ranging from 823 to 923 K in the rate of 10 K min^{-1} , which is remained for 20 min at each temperature. The catalysts reduction was performed in the hydrogen stream rate of 30 mL/min in 923 K at 3 h, and cooled slowly to 773 K under the Ar atmosphere with a flow rate of (30 mL/min). Finally, the gas composition of reactants, and products was recorded by using of HID YL-6100 GC with Carboxen 1010 column.

3. Results and discussions

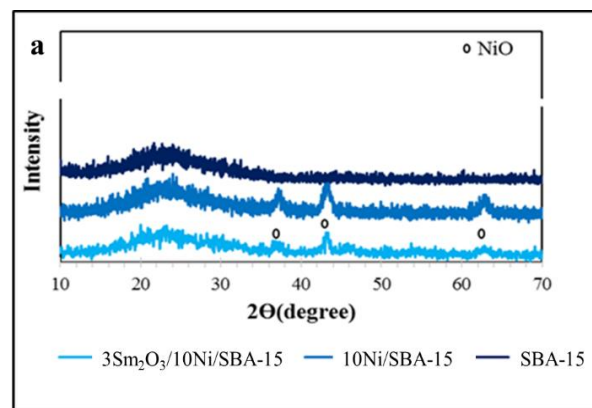
3.1. Evaluation of prepared catalysts

The high angle X-ray diffraction evaluation of the mesoporous SBA-15, CMK-3 as supports, unmodified Nickel-SBA-15, Nickel-CMK-3, modified Nickel-SBA-15. and Nickel-CMK-3 catalysts by Sm_2O_3 are presented in Fig. 2a and b. In Fig. 2a, for the SBA-15 a broad peak related to the amorphous silica observed and other three diffraction peaks, in range of $2\theta \approx 30^\circ\text{-}60^\circ$, for modified and unmodified Ni-SBA-15, as well, that is showing the incorporation of Nickel oxide particles into the SBA-15 channels (JCPDS 04-0835). It is considered that in Sm_2O_3 -Ni-SBA-15 catalyst, similar to unprompted Ni-SBA-15 sample, Nickel oxide diffraction peaks with lower intensities without diffraction peak of Sm_2O_3 are observed. Probably, the small particle size of samarium oxide or well dispersed of nanoparticles in the amorphous form on the surface of the support are out of XRD analysis detect [33]. In Fig. 2b, the XRD analysis of the CMK-3, Ni-CMK-3, and Sm_2O_3 -Ni/CMK-3 are observed, and similar to Fig. 1a, as the board peak is related to the mesoporous carbon, and the other intensive peaks are related to the Nickel oxide crystalline phase. The textural parameters of the promoted/unprompted Nickel catalysts over SBA-15, and CMK-3 are demonstrated in Table 1. The NiO crystalline average size for all catalysts is calculated from equation.(1):

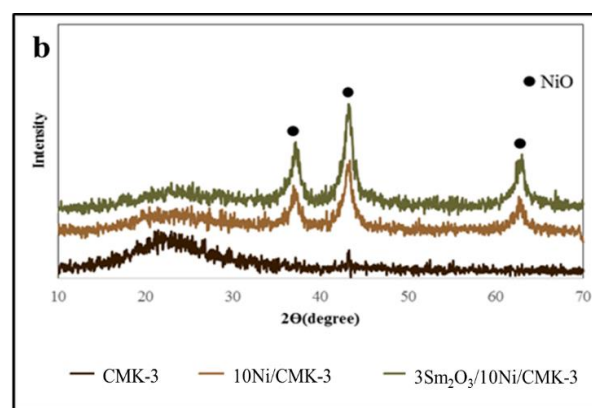
$$D = k\lambda/(\beta\cos\theta) \quad (1)$$

Where;

D represents the mean size of ordered (crystalline) domains, which may be smaller or equal to the grain size; K represents a dimensionless shape factor, with a value close to unity.



(a)



(b)

Figure 2. The x-ray diffraction patterns of a. SBA-15, 10Ni-SBA-15 and $3\text{Sm}_2\text{O}_3$ -10Ni-SBA-15, b. CMK-3, 10Ni-CMK-3 and $3\text{Sm}_2\text{O}_3$ -10Ni-CMK-3.

λ represents the X-ray wavelength;

β represents the line broadening at half the maximum intensity (FWHM) and θ is the Bragg angle.

In Fig. 3a, the pure SBA-15, is demonstrated an IV type isotherm with an H1-type hysteresis loop, which is corresponded to the IUPAC classification, and is related to mesoporous materials with cylindrical or hexagonal pores [34]. The observed sharp peak in the range of $P/P_0 = 0.5\text{-}0.75$ of isotherms (Fig. 3a); which are specifically capillary condensation within the uniform mesoporous. When Nickel and samarium are impregnated to SBA-15. Furthermore, the loop form is still preserved, that is demonstrating the similar structure in Ni-SBA-15 and Sm_2O_3 -Ni-SBA-15 catalyst.

Fig. 3b shows the considerable changes in the isotherms shape for CMK-3, Ni-CMK-3, and Sm_2O_3 -Ni-CMK-3 samples. As shown in Fig. 3b, the hysteresis loops have modified from a slim H1 type for SBA-15, 10 Ni/SBA-15, and Sm_2O_3 -Ni-SBA-15 catalysts to a broad H4 type for CMK-3, Ni-CMK-3, and Sm_2O_3 -Ni-CMK-3 samples. Also, the similar results have been previously published [28]. By comparison the results between BJH curves of promoted/unprompted Ni catalysts supported on SBA-15, and promoted/unprompted Ni catalysts supported on

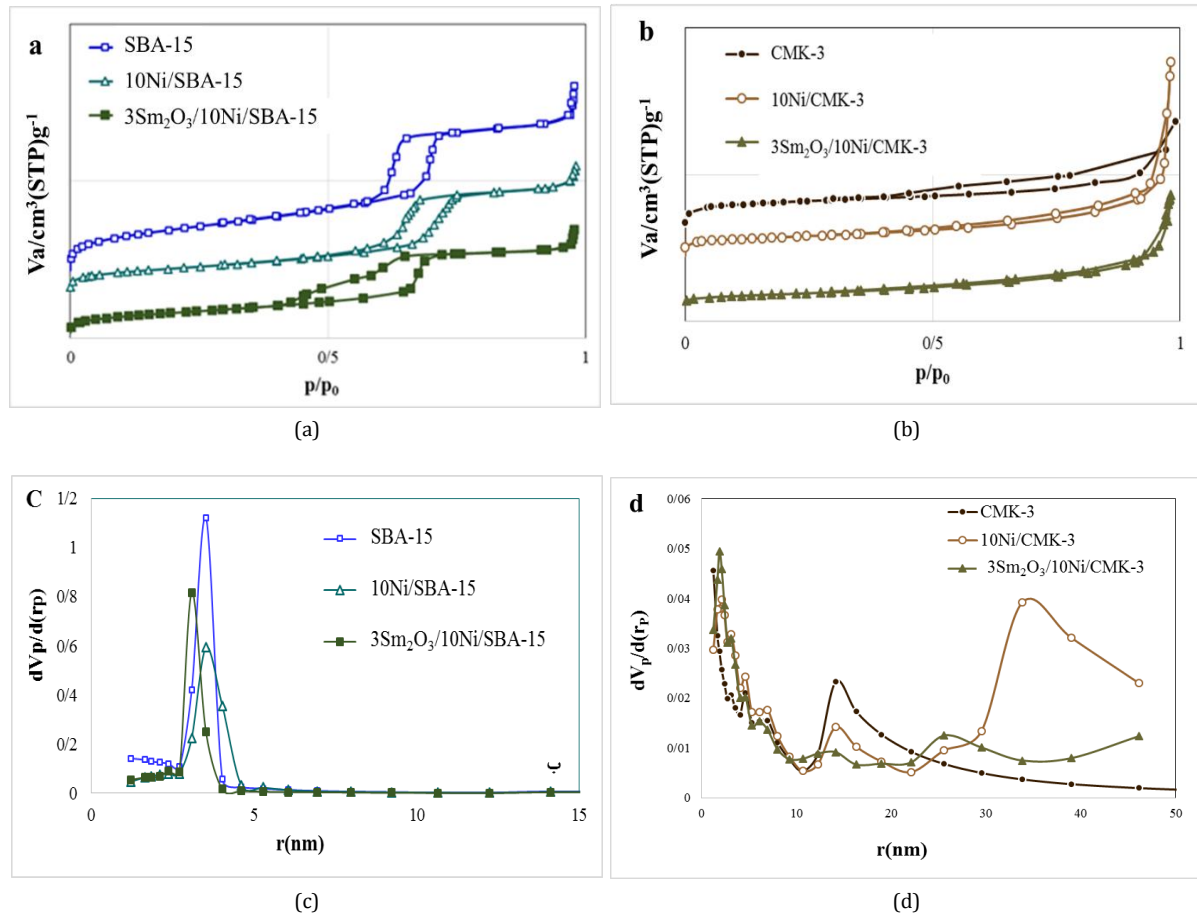


Figure 3. Adsorption-Desorption Isotherms for a. SBA-15, 10Ni-SBA-15, 3Sm₂O₃-10Ni-SBA-15, b. CMK-3, 10Ni-CMK-3, 3Sm₂O₃-10Ni-CMK-3, and BJH Adsorption and Pore Size Distribution for c.) SBA-15, 10Ni-SBA-15, 3Sm₂O₃-10Ni/SBA-15 and d) CMK-3, 10Ni-CMK-3, 3Sm₂O₃-10Ni-CMK-3.

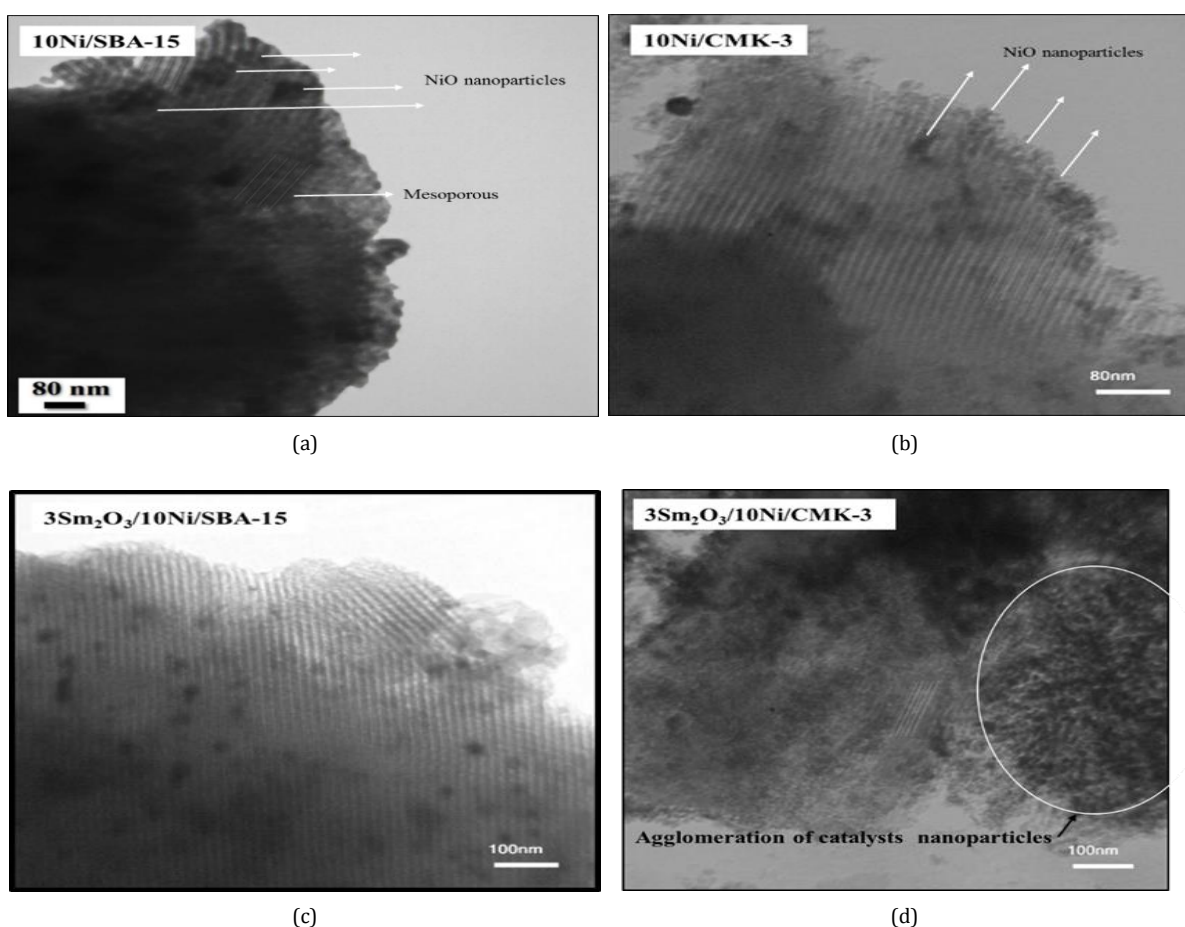
CMK-3 (Fig 3c and d), a narrow pore size distribution for Nickel-based catalysts over silica mesoporous and a broader pores size distribution for Nickel-based catalysts over the carbon mesoporous is revealed. These results are in agreement with the hysteresis type, e.g., for the Nickel catalysts over silica mesoporous. However the adsorption and desorption curves (hysteresis loops) are sharper than the pore-filling step in Ni catalysts supported on carbon mesoporous. As shown in Table 1, the result of textural properties such as; BET surface area, total pore volume, and average pore diameter are presented. According to Table 1 results, the surface area of SBA-15, and CMK-3 supports are approximately the same, while the pores volume and pores diameter of CMK-3 are lower than the SBA-15 support. In fact, the silica template has not entirely eliminated, and some of the silica has still remained inside the pores in the wall. Additionally, the decreasing of the modified/unmodified surface area of Nickel catalysts compared to supports, which is due to the blocking of pores after impregnating Ni and Sm₂O₃ into the SBA-15, and CMK-3 supports. For instance, the surface area of Ni-SBA-15, and Ni-CMK-3 catalysts is decreased from 780 m²/g to 400 and 313 m²/g. And the

surface area of Sm₂O₃-Ni-SBA-15, and Sm₂O₃-Nickel-CMK-3 is reduced from 780 m²/g to 422 and 154 m²/g, respectively. As a result, the addition of Sm₂O₃ as a promoter to Ni-SBA-15, and Ni-CMK-3 samples is decreases the pore volume, that is indicating that some of the Samaria nanoparticles have located inside the pores.

For getting more information about the structural order and nanoparticles dispersion over the modified/unmodified Nickel catalysts over SBA-15, and CMK-3, TEM micrographs are done. Fig.4 shows the TEM images of all prepared catalysts. In sample of Ni/SBA-15, and Samaria-incorporated Ni/SBA-15 catalysts, the uniform channels of mesoporous are clearly observed, that is showing well-ordered SBA-15 structure after adding Samaria. It can also be seen in Fig. 4, the modified/unmodified Ni catalysts with the Samaria supported on mesoporous carbon materials (CMK-3) indicate a less ordered structure. These outcomes are agree with the recorded results in Table 1, that is indicating that the larger pores diameter in Sm₂O₃/Ni/CMK-3 catalyst leads to more located Nickel oxide, and Samaria inside the pores and causes the reduction of structural order, surface area, and pores volume. By comparing the TEM images of

Table 1. Textural properties of the support and with/without promoter catalysts.

Sample	SBA-15	10Ni/SBA-15	3Sm ₂ O ₃ /10Ni/SBA-15	CMK-3	10Ni/CMK-3	3Sm ₂ O ₃ /10Ni/CMK-3
BET surface area (m ² /g)	781.7	401	422.9	781	313.2	154
Pore volume (ml/g)	1.39	0.93	0.8	0.73	1.05	0.58
Pore diameter (nm)	7.14	9.3	7.58	3.8	13.5	15.28
NiO particle size (nm)	-	8.95	7.26	-	8.43	8.62
%Dispersion	-	11.2	13.8	-	11.8	11.6

**Figure 4.** TEM micrographs of 10Ni-SBA-15, 10Ni-/CMK-3, 3Sm₂O₃-10Ni/SBA-15 and 3Sm₂O₃-10Ni-CMK-3.

Samaria promoted Nickel catalysts over SBA-15, and CMK-3. And it can be resulted that the spherical Nickel particles are smaller, and the more dispersed (dark regions) inside the mesoporous channels of SBA-15 with a dispersion of 13.8% than Samaria promoted Ni catalysts supported on CMK-3 with a dispersion of 11.2% (Table

1). These observations are according to XRD and BET characterization results.

The FE-SEM image, and EDAX analysis of 3Sm₂O₃/10Ni/CMK-3 catalyst (Fig.5) confirms the presence of C, Ni and Sm related to support, catalyst and promoter, respectively.

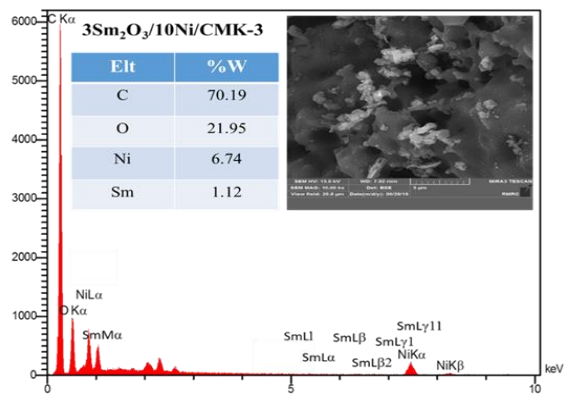
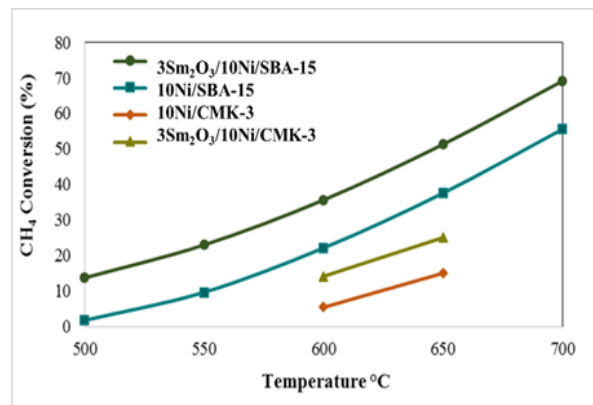


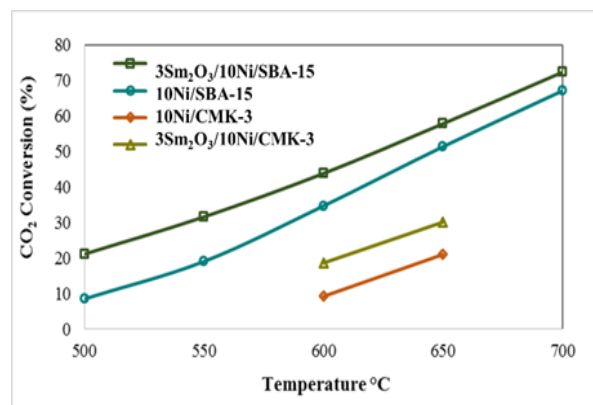
Figure 5. FESEM image and EDS analysis of $3\text{Sm}_2\text{O}_3\text{-}10\text{Ni-CMK-3}$.

3.2. Catalytic activity

For studying the catalytic performance, before catalytic tests, the reduction process was performed in a stream of hydrogen gas (30 mL/min) at 923 K (10 K/min) at 3 h in all calcined samples. Because, Yousefpour *et al.*, previously reported that the Nickel oxide completely changed to Ni_0 at this temperature [1, 2]. When, catalysts reduction is completed, the temperature is reduced to 723 K, and the hydrogen stream is changed to methane, and carbon dioxide flows with ratio of 1:1, and injected to the reactor with a total stream rate at 40 mL/min. The methane, and carbon dioxide conversions were evaluated simultaneously with temperature raising from 723 to 923 K. The total Gas Hourly Space Velocity (GHSV) was selected 1.2 L/g h. Fig. 6 demonstrates the samples methane, and carbon dioxide conversions against the temperature. It can be seen, as the reaction temperature rises, methane and carbon dioxide conversions enhances as well. The catalytic behavior revealed that the activation of Nickel catalysts with and without the Samaria supported on SBA-15 started at 723 K, and reached to the maximum activity at 1023 K. However, the activation of Nickel catalysts with/without the Samaria supported on CMK-3 appeared above 874 k with low values and ended at 923 K. Furthermore, fig. 6 shows the higher CO_2 conversion than CH_4 conversion for all catalysts. As can be seen in Fig 6, the adding Samaria as promoter increases the catalysts activity of Nickel catalysts over SBA-15, and CMK-3 in comparison to the unprompted Ni catalysts, that is related to the redox properties of Samaria due to improve the chemisorption of carbon dioxide, and transition of oxygen [35]. Adding the Sm_2O_3 showed a significant effect on the better catalysts efficiency. Additionally, the effect of the support on the catalyst activity is obvious in Fig.6, where the higher activities is related to the Samaria promoted, and unprompted Ni catalysts supported on the SBA-15 than supported on the CMK-3. Since the nature of mesoporous carbon is basic, thus it is expected the activity of Ni catalysts supported on the CMK-3 will be higher in dry reforming of methane. On the other hand, Goscianska *et al.* [28], previously reported the higher activity of La



(a)



(b)

Figure 6. CH_4 conversion and CO_2 conversion dependence on reaction temperature over Samaria promoted and unprompted Ni-based catalysts supported on SBA-15 and CMK-3. Conditions: $\text{GHSV}=12000\text{ml}/(\text{h.g}_{\text{cat}})$, $\text{CO}_2/\text{CH}_4=1:1$, $P=1\text{atm}$.

and Ce/CMK-3 with higher basic groups than La and Ce/SBA-15 at 923 k in the carbon dioxide reforming of CH_4 reaction. In the present study, the probably negative role of the CMK-3 as a support for Ni catalyst is due to the agglomeration of NiO nanoparticles into CMK-3 channels (as seen in the TEM images), and the lower surface area (According to the BET result in Table. 1), and the calcination of Nickel/CMK-3 catalysts during the impregnation process for the several times.

3.3. Catalysts stability study

Fig.7 shows the short stability of all catalysts at 923 K for 300 min of reaction. In our previous research [1, 2], for the promoted and unprompted Ni catalysts supported on SBA-15, enough stability at 923 K for 900 min during of reaction obtained. In the present study, the Ni catalysts supported on mesoporous silica show more stability at 923 K, but the promoted, and unprompted Ni/CMK-3 catalysts did not show enough stability compared to the promoted Ni catalyst.

On the other hand, the carbon mesoporous as support is not stable at temperatures above 923 K, and it is

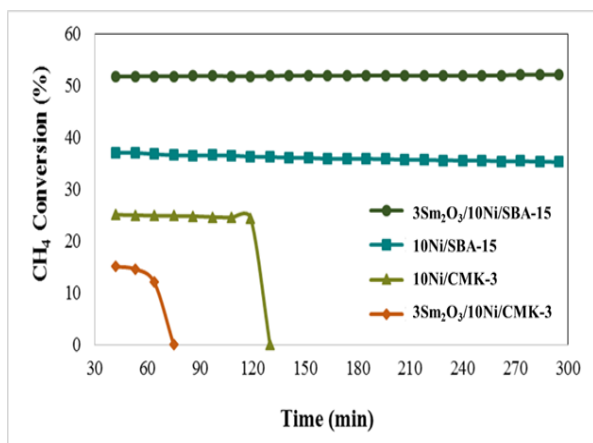


Figure 7. The short stability of Samaria promoted/unpromoted Ni catalysts supported on SBA-15 and CMK-3. 923 k for 300 min. Conditions: GHSV=12000ml/(h.g_{cat}), CO₂/CH₄=1:1, P=1atm and T=923 k.

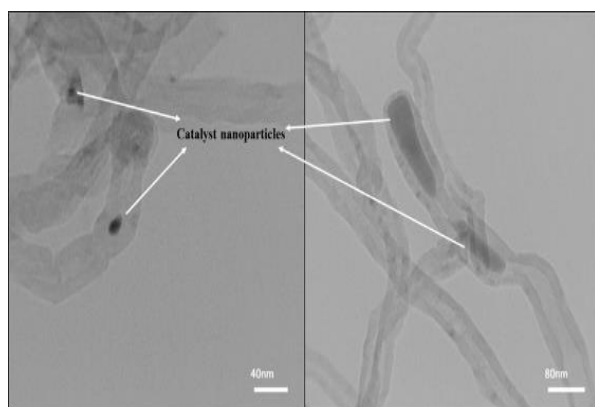


Figure 8. The TEM micrographs of used Samaria promoted Ni/CMK-3.

evaporated and deactivated by rapid oxidation. However, after adding Samaria to Ni/CMK-3 catalyst, the catalyst stability increases to about two hours, and then it is suddenly deactivated. Probably, the formation of the middle phase of Nickel-Samarium with a strong interaction with the support leads to a higher thermal stability of the barrier. The reason for the rapid deactivation of these catalysts can be attributed to various factors such as particles sintering of the catalyst, the carbon deposition (as seen in Fig.8), and catalyst oxidation has happened at the higher temperatures of reaction. Although in prior studies, it has not been published any report about the Nickel catalysts supported on CMK-3 in the methane reforming in expose to carbon dioxide, however recently, similar results has been published about the stability of the La and Ce catalysts supported on the carbon mesoporous after one or two hours at 923 K [28].

Fig. 8 demonstrates the TEM images of deposited carbon during the dry reforming of methane reaction before the completely burning. It is clear that the nanotubes from the carbon deposited on Sm₂O₃/Nickel/CMK-3 surface. The dark spots inside the nanotubes indicate the Ni particles blocked into the nanotubes carbon, and no expose in feed gases that can be

the main reason for rapid deactivation of the Ni catalysts supported on the carbon mesoporous. However, it had been reported that the deposited carbon over the Sm₂O₃/10Nickel/SBA-15 catalyst was a tip type carbon and Ni active sites on the support surface remained in exposing to the feed gases and revealed slow deactivation compared to Sm₂O₃/Nickel/CMK-3 catalyst.

Conclusion

The hexane-solvent impregnation technique was a successful way for synthesis of the Samaria promoted Nickel catalysts over CMK-3 barriers. According to the XRD results, the 3Sm₂O₃/10Ni/SBA-15 sample showed the higher dispersion and lower particle size of NiO nanoparticles compared to the Sm₂O₃/Nickel/CMK-3. The BET outcomes revealed that the addition of Samaria reduced the specific surface area of Nickel supported on the SBA-15S, and CMK-3. The TEM images of fresh catalysts indicated that the agglomeration of nanoparticles into the CMK-3 channels occurred after the incorporating of Samaria. The dry reforming revealed that the incorporation of Samaria has a positive role in catalysts activity, while the use of CMK-3 as a support plays a negative role in Ni catalysts compared to SBA-15. The main reasons for lower stability of Ni catalysts supported on the CMK-3 can be related to the agglomeration of Ni nanoparticles on the support surface, the deposition of nanotubes carbon on the catalyst surface and blocking of the Ni particles, and instability of the CMK-3 support in a high

Acknowledgements

Authors, gratefully thank Semnan University for partial research support.

References

- [1] Z. Taherian, M. Yousefpour, M. Tajally, B. Khoshandam, Promotional effect of samarium on the activity and stability of Ni-SBA-15 catalysts in dry reforming of methane, *Microporous and Mesoporous Materials*, 251, 9-18, (2017)
- [2] Z. Taherian, M. Yousefpour, M. Tajally, B. Khoshandam, A comparative study of ZrO₂, Y₂O₃ and Sm₂O₃ promoted Ni/SBA-15 catalysts for evaluation of CO₂/methane reforming performance. *International Journal of Hydrogen Energy*, 42(26), 6408-1642, (2017).
- [3] Z. Taherian, M. Yousefpour, M. Tajally, B. Khoshandam, Catalytic performance of Samaria-promoted Ni and Co/SBA-15 catalysts for dry reforming of methane, *International Journal of Hydrogen Energy*, 42(39), 24811-24822, (2017).

- [4] S. Das, M. Sengupta, J. Patel, A. Bordoloi, A study of the synergy between support surface properties and catalyst deactivation for CO₂ reforming over supported Ni nanoparticles. *Applied Catalysis A: General*, 545, 113-126, (2017).
- [5] T.S. Phan, A.R. Sane, B.R. Vasconcelos, A. Nzihou, P. Sharrock, D. Grouset, D. P. Minh, Hydroxyapatite supported bimetallic cobalt and Nickel catalysts for syngas production from dry reforming of methane. *Applied Catalysis B: Environmental*, 224, 310-321, (2018).
- [6] E. Rbib, H.C. Bouallou, F. Werkoff, Production of synthetic gasoline and diesel fuel from dry reforming of methane, *Energy Procedia*, 29, 156-165, (2012).
- [7] M. Sarkari, F. Fazlollahi, H. Atashi, A.A. Mirzaei, W.C. Hecker, Using different preparation methods to enhance Fischer-Tropsch products over iron-based catalyst, *Chemical and biochemical engineering quarterly*, 27(3), 259-266, (2013).
- [8] S. Yasyerli, S. Filizgok, H. Arbag, N. Yasyerli, G. Dogu, Ru incorporated Ni-MCM-41 mesoporous catalysts for dry reforming of methane: Effects of Mg addition, feed composition and temperature, *International Journal of Hydrogen Energy*, 36(8), 4863-4874, (2011).
- [9] N. El Hassan, M.N. Kaydouh, H. Geagea, H. Elein, K. Jabbour, S. Casale, H E. Zakhem, Pascale Massiani, Low temperature dry reforming of methane on rhodium and cobalt based catalysts: active phase stabilization by confinement in mesoporous SBA-15, *Applied Catalysis A: General*, 520, 114-121(2016).
- [10] S. Damyanova, B. Pawelec, K.A. Arishtirova, J.L.G. Fierro, C. Sener, T. Dogu, MCM-41 supported PdNi catalysts for dry reforming of methane. *Applied Catalysis B: Environmental*, 92(3-4), 250-261, (2009)..
- [11] M.G. Diéguez, E. Finocchio, M.Á. Larrubia, L.J. Alemany, G. Busca, Characterization of alumina-supported Pt, Ni and PtNi alloy catalysts for the dry reforming of methane, *Journal of Catalysis*, 274(1), 11-20, (2010).
- [12] E. Steinhauer, M.R. Kasireddy, J. Radnik, A. Martin, Development of Ni-Pd bimetallic catalysts for the utilization of carbon dioxide and methane by dry reforming, *Applied Catalysis A: General*, 366(2), 333-341, (2009).
- [13] W. Gac, W. Zawadzki, G. Słowik, A. Sienkiewicz, A. Kierys, Nickel catalysts supported on silica microspheres for CO₂ methanation, *Microporous and Mesoporous Materials*, 272, 7-17, (2018)
- [14] M.S. Lanre, A.S. Al-Fatesh, A.H. Fakeeh, S.O. Kasim, A.A. Ibrahim, A.S. Al-Awadi, A.A. Al-Zahrani, A.E. Abasaed, Effects of preparation technique and lanthana doping on Ni/La₂O₃-ZrO₂ catalysts for hydrogen production by CO₂ reforming of coke oven gas. *Catalysis Today*, 318(15), 23-31, (2017).
- [15] S.Wang, Y. Wang, C. Hu, The effect of NH₃-H₂O addition in Ni/SBA-15 catalyst preparation on its performance for carbon dioxide reforming of methane to produce H₂, *International Journal of Hydrogen Energy*, 30(26), 13921-13930, (2018).
- [16] B. Fidalgo, L. Zubizarreta, J.M.B. Menendez, A. Arenillas, J.A. Menéndez, Synthesis of carbon-supported Nickel catalysts for the dry reforming of CH₄, *Fuel Processing Technology*, 91(7), 765-769, (2010).
- [17] J. Matos, K. Díaz, V. García, T.C. Cordero, J.L. Brito, Methane transformation in presence of carbon dioxide on activated carbon supported Nickel-calcium catalysts, *Catalysis letters*, 109(3), 163-169, (2006).
- [18] K. Díaz, V. García, J. Matos, Activated carbon supported Ni-Ca: influence of reaction parameters on activity and stability of catalyst on methane reformation, *Fuel*, 86(9), 1337-1344, (2007).
- [19] M.C.Bradford, M.A. Vannice, Catalytic reforming of methane with carbon dioxide over Nickel catalysts I. Catalyst characterization and activity, *Applied Catalysis A: General*, 142(1), 73-96, (1996).
- [20] B. Fidalgo, J.Á. Menendez, Carbon materials as catalysts for decomposition and CO₂ reforming of methane: a review, *Chinese journal of catalysis*, 32(1-2), 207-216, (2011).
- [21] A. Dandekar, R. Baker, M. Vannice, Carbon-supported copper catalysts: I. Characterization, *Journal of Catalysis*, 183(1), 131-154, (1999).
- [22] N.B. Klinghoffer, M.J. Castaldi, A. Nzihou, Catalyst properties and catalytic performance of char from biomass gasification, *Industrial & Engineering Chemistry Research*, 51(40), 13113-13122, (2012).
- [23] V.L. Budarin, J.H. Clark, S.J. Tavener, K. Wilson, Chemical reactions of double bonds in activated carbon: microwave and bromination methods, *Chemical Communications*, 23, 2736-2737, (2004).
- [24] L. Xu, Y. Liu, Y. Li, M. Fan, Catalytic CH₄ reforming with CO₂ over activated carbon based catalysts. *Applied Catalysis A: General*, 469, 387-397, (2014).
- [25] Y. Shen, A.C. Lu, A trimodal porous carbon as an effective catalyst for hydrogen

- production by methane decomposition, *Journal of colloid and interface science*, 462, 48-55, (2016).
- [26] F. Rodriguez-Reinos, The role of carbon materials in heterogeneous catalysis. *Carbon*, 36(3), 159-175, (1998). 27. F. Stüber, J. Font, A. Fortuny, C. Bengoa, A. Eftaxias, A. Fabregat, Carbon materials and catalytic wet air oxidation of organic pollutants in wastewater, *Topics in Catalysis*, 33(1-4), 3-50, (2005).
- [28] J. Goscińska, R. Pietrzak, J. Matos, Catalytic performance of ordered mesoporous carbons modified with lanthanides in dry methane reforming, *Catalysis Today*, 301, 204-216, (2018).
- [29] D. Zhao, J. Sun, Q. Li, G.D. Stucky, Morphological control of highly ordered mesoporous silica SBA-15. *Chemistry of Materials*, 12(2), 275-279, (2000).
- [30] S. Jun, S.H. Joo, R. Ryoo, M. Kruk, M. Jaroniec, Z.H. Liu, T. Ohsuna, O. Terasaki, Synthesis of new, nanoporous carbon with hexagonally ordered mesostructure. *Journal of the American Chemical Society*, 122(43), 10712-10713, (2000).
- [31] M.I. Clerc, D. Bazin, M.D. Appay, P. Beaunier, A. Davidson, Crystallization of β -MnO₂ nanowires in the pores of SBA-15 silicas: in situ investigation using synchrotron radiation, *Chemistry of materials*, 16(9), 1813-1821, (2004).
- [32] M.N. Kaydouh, N.E. Hassan, A. Davidson, S. Casale, H.E. Zakhem, P. Massian, Highly active and stable Ni/SBA-15 catalysts prepared by a "two solvents" method for dry reforming of methane, *Microporous and Mesoporous Materials*, 220, 99-109, (2016).
- [33] J.F. Li, C. Xia, C.T. Au, B.S. Liu, Y₂O₃-promoted NiO/SBA-15 catalysts highly active for CO₂/CH₄ reforming, *International Journal of Hydrogen Energy*, 39(21), 10927-10940. (2014).
- [34] M.A. Azizi Ganzaghi, M. Yousefpour, Z. Taherian, The removal of mercury (II) from water by Ag supported on nanomesoporous silica, *Journal of chemical biology*, 9(4), 127-142, (2016).
- [35] V. Shanmugam, R. Zapf, S. Neuberg, V. Hessel, G. Kolb, Effect of ceria and zirconia promoters on Ni/SBA-15 catalysts for coking and sintering resistant steam reforming of propylene glycol in microreactors. *Applied Catalysis B: Environmental*, 203, 859-869.